

All-Conjugated Block Copolymers

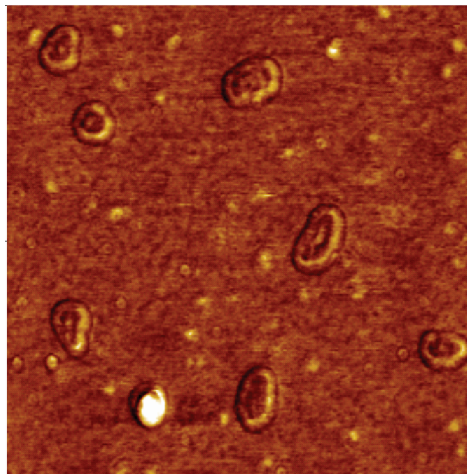
ULLRICH SCHERF,* ANDREA GUTACKER, AND NILS KOENEN
Macromolecular Chemistry Group, Department of Chemistry, and Institute for
Polymer Technology, Bergische Universität Wuppertal, Gauss-Strasse 20,
D-42097 Wuppertal, Germany

RECEIVED ON NOVEMBER 21, 2007

CONSPECTUS

All-conjugated block copolymers of the rod–rod type came into the focus of interest because of their unique and attractive combination of nanostructure formation and electronic activity. Potential applications in a next generation of organic polymer materials for photovoltaic devices (“bulk heterojunction”-type solar cells) or (bio)-sensors have been proposed. Combining the fascinating self-assembly properties of block copolymers with the active electronic and/or optical function of conjugated polymers in all-conjugated block copolymers is, therefore, a very challenging goal of synthetic polymer chemistry. First examples of such all-conjugated block copolymers from a couple of research groups all over the world demonstrate possible synthetic approaches and the rich application potential in electronic devices.

A crucial point in such a development of novel polymer materials is a rational control over their nanostructure formation. All-conjugated di- or triblock copolymers may allow for an organization of the copolymer materials into large-area ordered arrays with a length scale of nanostructure formation of the order of the exciton diffusion length of organic semiconductors (typically ca. 10 nm). Especially for *amphiphilic*, all-conjugated copolymers the formation of well-defined supramolecular structures (vesicles) has been observed. However, intense further research is necessary toward tailor-made, all-conjugated block copolymers for specific applications. The search for optimized block copolymer materials should consider the electronic as well as the morphological (self-assembly) properties.



Introduction

The synthesis and self-assembling behavior of all-conjugated rod–rod block copolymers is still a very challenging area in the field of polymer chemistry. Moreover, it is a territory with high application potential, e.g. as photovoltaic materials, biosensors etc.¹ Emerging applications for conjugated (co)polymers in organic photovoltaics (organic solar cells) and biotechnology (biosensors) often require the patterning of materials on the 10–100 nm length scale, and block copolymers may provide an elegant route to control the self-assembly into such nanostructured morphologies. However, the rodlike nature of most conjugated polymers complicates the self-assembly of corre-

sponding block copolymers through a competition between crystalline and liquid crystalline interactions and the nanophase separation.

To realize highly ordered, nanostructured films a certainly high molecular weight of the individual blocks and, especially, a narrow molecular weight distribution are preferred. However, it is a great synthetic challenge to generate all-conjugated block copolymers because conventional synthetic methods, especially living anionic polymerization, most often cannot be applied for conjugated polymer synthesis. Very recently first reports on a polydispersity control for polycondensation schemes toward polythiophenes, polyphenylenes and polyfluorenes have been published.²

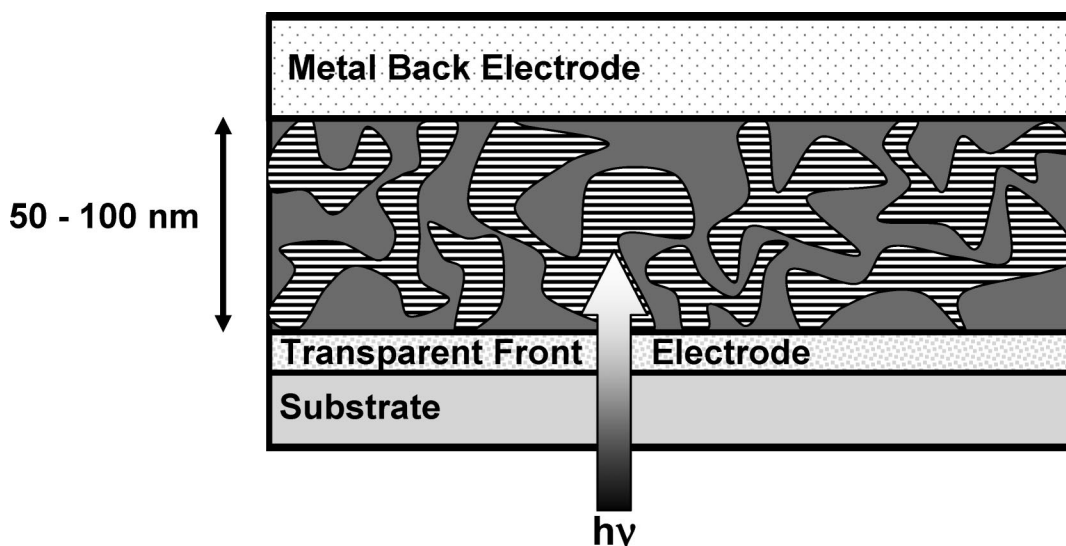


FIGURE 1. Schematic device structure of a “bulk heterojunction”-type organic solar cell based on a phase-separated donor/acceptor couple; nanoscopic mixing of donor and acceptor components helps to overcome the very short exciton diffusion length in organic (disordered) semiconductors (~ 10 nm).

All-Conjugated Block Copolymers. The number of publications on all-conjugated rod–rod block copolymers is limited; only a few reports have been published. In a series of research reports Sun et al. have described poly(phenylene vinylene) (PPV)-based block copolymers with PPV blocks of different electron density by connecting electron rich poly(2,5-dialkoxyphenylene vinylene) “donor” and poly(2-alkylsulfonyl-5-alkoxyphenylene vinylene) “acceptor” blocks.^{3,4} A nanostructure formation on a length scale of 10–20 nanometers with separated donor and acceptor phases was postulated. The block copolymers have been applied as active layers in “bulk heterojunction”-type organic solar cells (for the schematic design of a “bulk heterojunction”-type organic solar cell see Figure 1) and have been discussed in comparison to the corresponding polymer blends with their noncontrolled microphase separation.^{5,6} The controlled nanophase formation of all-conjugated donor/acceptor block copolymers is very attractive in relation to the short exciton diffusion lengths of organic semiconductors of ca. 10 nm.^{7–9} The HOMO and LUMO energy levels of the donor/acceptor couple of an organic solar cell (HOMO, highest occupied molecular orbital; LUMO, lowest unoccupied molecular orbital) together with the electron (charge) flow from the anode to the cathode are illustrated in Figure 2.

Related all-conjugated diblock oligomers have been described by Yu et al.¹⁰ The diblock oligomers contain nonpolar oligo(2,5-dialkylphenylene vinylene) (OPV) and oligo(3-alkylthiophene) (O3AT) blocks. Excitation energy transfer from the higher bandgap OPV to the lower bandgap O3AT blocks was observed after excitation into the OPV absorption band.

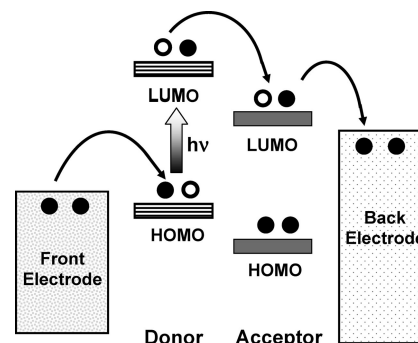
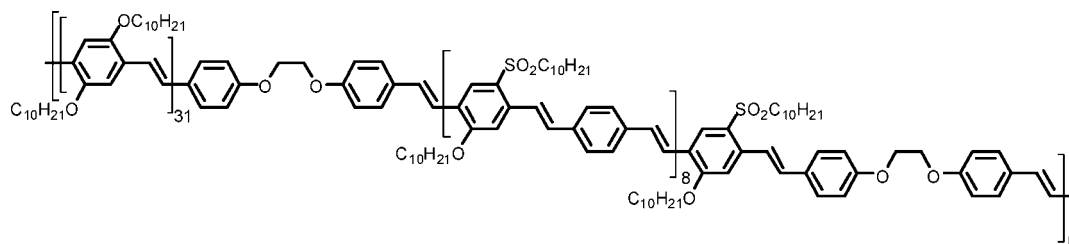
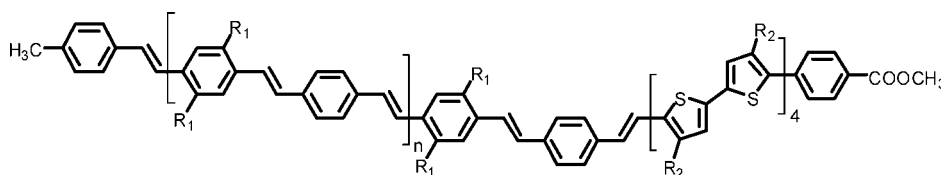


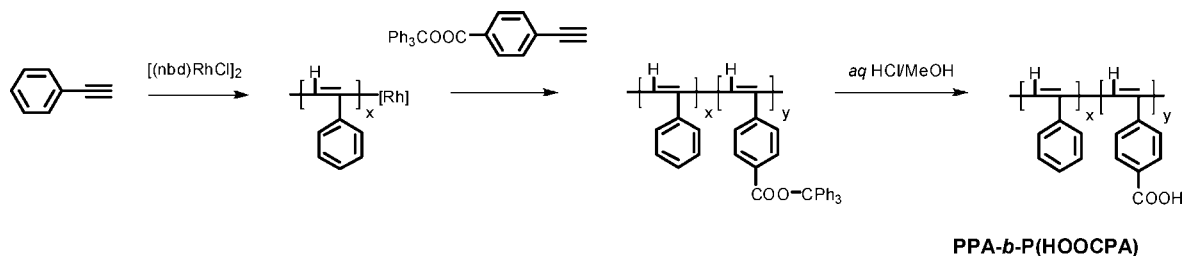
FIGURE 2. Energy levels of the active donor/acceptor couple of an organic solar cell; the electron flow from the anode (front electrode) to the cathode (back electrode) is illustrated ($h\nu$ represents the incoming solar energy).

The diblock oligomers self-assemble into fibrils or lamellar nanostructures.

Two early reports on all-conjugated block copolymers were published in 2001. The Masuda group from Kyoto described poly(phenylacetylene) (PPA)-based diblock copolymers with polar poly(4-carboxyphenylacetylene) and nonpolar poly(phenylacetylene) blocks.¹¹ The living polymerization of the phenylacetylene monomers with Rh catalysts produces diblock copolymers with a very narrow molecular weight distribution of M_w/M_n : ~ 1.1 (Schemes 1,2,3). The amphiphilic poly(phenylacetylene)-*b*-poly(4-carboxyphenylacetylene) [PPA-*b*-P(HOOCPA)] diblock copolymers are soluble in DMSO or DMF as nonselective solvents. Addition of selective solvents for one of the blocks [benzene for the nonpolar PPA block; water for the polar poly(4-carboxyphenylacetylene) block] leads to the formation of core/shell aggregates, most probably micelles

SCHEME 1. Structure of Donor/Acceptor Block Copolymers Poly(2,5-didecyloxyphenylene vinylene)-*b*-poly(2-decylsulfonyl-5-decyloxyphenylene vinylene) after Sun et al⁶**SCHEME 2.** Structure of All-Conjugated Diblock Cooligomers Oligo(2,5-dialkylphenylene vinylene)-*alt*-phenylene vinylene)-*b*-oligo(3-alkylthiophene) (OPV-*b*-O3AT) after Yu et al^{1,10 a}

^a *n*: 1, 2, 4. R₁: *n*-hexyl. R₂: 2-ethylhexyl.

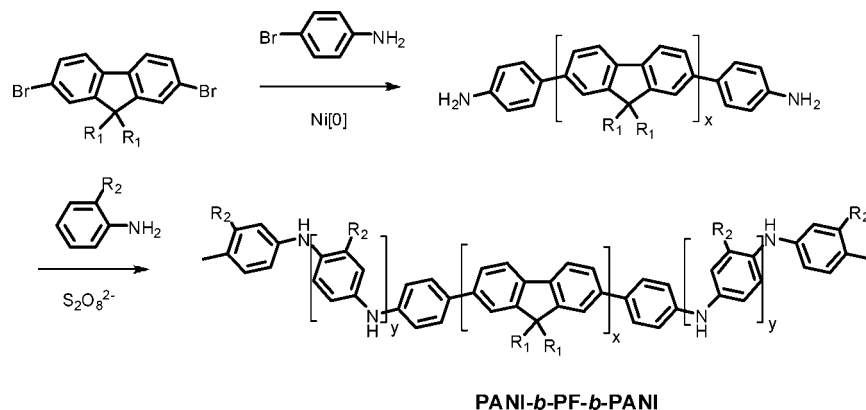
SCHEME 3. Synthesis of Poly(phenylacetylene)-*b*-poly(4-carboxyphenylacetylene) Diblock Copolymers in a Living Polymerization after Masuda et al¹¹

due to a NMR analysis. The diblock copolymers form Langmuir–Blodgett (LB) monolayers at the air/water interface.

An all-conjugated rod–rod-type block copolymer poly(9,9-dialkyl)fluorene-*block*-poly(2-alkylaniline) was reported by us in a couple of papers starting from 2001.^{12–15} Hereby, a 4-aminophenyl end-functionalized polyfluorene (PF) precursor was generated in the first step. This was accomplished in a Yamamoto-type aryl–aryl coupling of 2,7-dibromo-9,9-dialkylfluorene using 1-bromo-4-nitrobenzene or 4-bromoaniline as monofunctional end-capping reagent (“end-capper”) to attach defined terminal functions at the polymeric precursor (Scheme 4). In the case of the 4-nitrophenyl “end-capper” a subsequent reduction to aminophenyl functions is necessary. The next step of the synthetic sequence is the generation of two terminal poly(2-undecylaniline) blocks in a “grafting-from” protocol starting at the aminoaryl terminals in an oxidative polycondensation with 2-undecylaniline. The term “grafting from” reflects the stepwise growth of the poly-aniline blocks at the terminals of the end-functionalized precursor. This synthetic sequence produces the final ABA-type

rod–rod triblock copolymer poly(2-undecylaniline)-*b*-poly[9,9-dialkylfluorene]-*b*-poly(2-undecylaniline) [PANI-*b*-PF-*b*-PANI] (Scheme 4).

The molecular weights of both blocks can be controlled by the feed ratios of monomers, end-cappers and prepolymers. The separation of block copolymers and homopolymer side products is accomplished by solvent extractions, since all components of the reaction mixture showed a rather different solubility behavior. The formation of block copolymers was proven by GPC measurements with UV–vis detection at the distinctly different absorption maxima of both blocks (PF block, ca. 380 nm, no absorption at wavelengths > 420 nm; PANI block, 550 nm). The resulting block copolymers show a spontaneous formation of branched, cylindrical nanostructures. The diameter of the structures varies between 50 and 300 nm, depending from the length of the solubilizing side groups, the molecular weights of the block copolymer and its composition, and the solvent system used (Figure 3). The film forming properties of the block copolymers have been studied by List and co-workers.^{14,15}

SCHEME 4. Synthesis of Poly(2-undecylaniline)-*b*-poly[9,9-dialkylfluorene]-*b*-poly(2-undecylaniline) (PANI-*b*-PF-*b*-PANI) Triblock Copolymers^a

^a R₁: -2-ethylhexyl or 3,7,11-trimethyldodecyl. R₂: -*n*-undecyl.

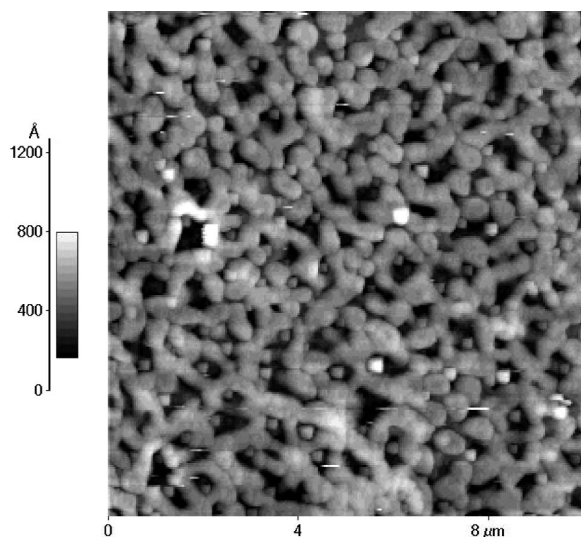
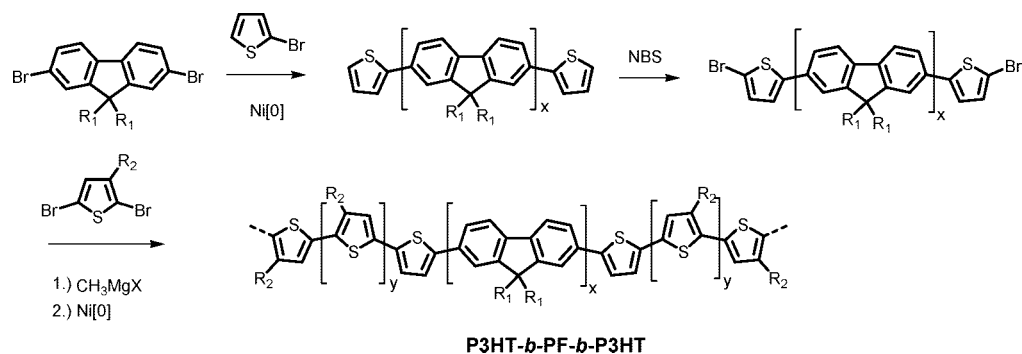


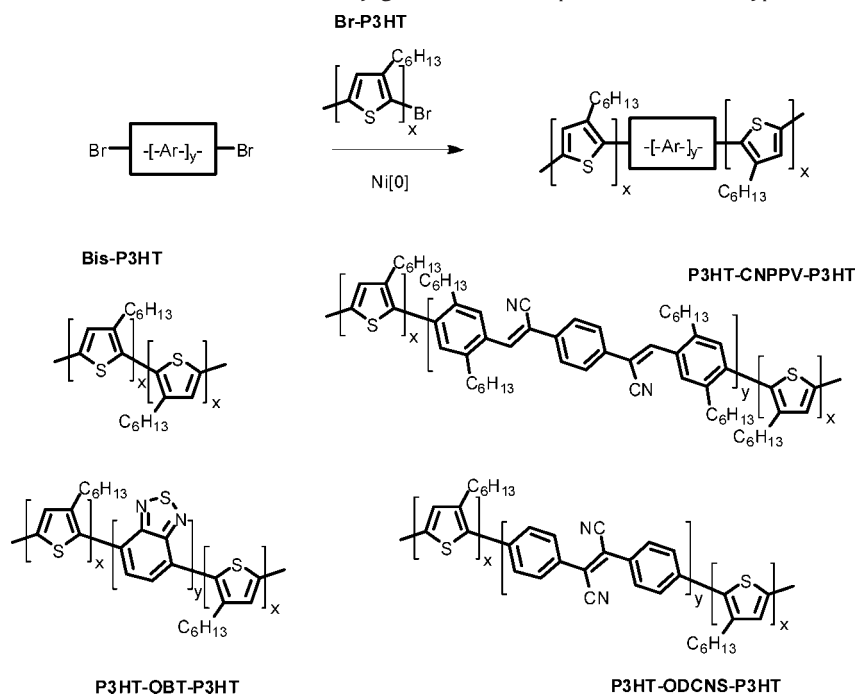
FIGURE 3. AFM image (topography mode) of a spin coated film of a triblock copolymer poly(2-undecylaniline)-*b*-poly[9,9-dialkylfluorene]-*b*-poly(2-undecylaniline) (PANI-*b*-PF-*b*-PANI) onto a glass slide.

Later, the synthetic methodology was adapted for the synthesis of poly(3-hexylthiophene)-*b*-poly[9,9-dialkylfluorene]-*b*-poly(3-hexylthiophene) triblock copolymers [P3HT-*b*-PF-*b*-P3HT] (Scheme 5).¹⁶ Here, 2-bromothiophene was used as monofunctional “end-capper” in the PF synthesis, followed by a bromination of the 2-thienyl terminals in the reactive 5-positions. Subsequent poly(3-hexylthiophene) (P3HT) synthesis via a so-called Grignard metathesis (GRIM) procedure after McCullough produces the ABA-type block copolymers. Again, side products (P3HT homopolymer) can be removed by solvent extraction. Interestingly, the block copolymers show a limited intramolecular excitation energy transfer from the higher (PF) to the lower bandgap (P3HT) blocks after excitation into the PF absorption band. In the solid state, however, a complete intermolecular energy transfer is observed.

The poly(9,9-dialkylfluorene)/poly(3-alkylthiophene) couple represents a typical energy transfer system (with two components with high and low bandgap energy, respectively). However, for a potential future application in “bulk heterojunction”-type organic solar cells combinations of electron-rich (donor) and electron-poor (acceptor) blocks are of primary importance for obtaining an efficient interfacial charge transfer (for the energy levels of such a couple see Figure 2).^{5,6} In 2006 we reported a straightforward two-step synthesis toward all-conjugated donor/acceptor/donor (DAD)-type triblock copolymers with both electron-donor (D) and electron-acceptor (A) blocks (Scheme 4).¹⁷ Hereby, cyano-substituted poly(phenylene vinylene) (CNPPV), oligo(benzothiadiazole) (OBT) and oligo(dicyanostilbene) (ODCNS) prepolymers with two bromoaryl terminals act as the central electron-acceptor (A) building block and are generated under Yamamoto-type aryl-aryl-coupling conditions. In a “grafting-onto” approach the dibromo-functionalized acceptor prepolymers are finally decorated with two regioregular poly(3-hexylthiophene) (P3HT) blocks in a coupling with monobromo-terminated Br-P3HT macromonomers (Scheme 6), which have been selected as the electron-donor block (D). The molecular weight of the different blocks can be controlled by adjusting the polymerization time and the substitution pattern (degree of alkyl substitution) of the monomers and macromonomers. Elemental analysis, NMR, DSC, and optical spectroscopy indicate the existence of DAD-type all-conjugated triblock copolymers. Atomic force microscopy (AFM) images of one triblock copolymer (P3HT-*b*-CNPPV-*b*-P3HT) exhibit the formation of regular nanosized mesostructures in thin films. The conjugated triblock copolymer P3HT-*b*-CNPPV-*b*-P3HT shows a distinctly different morphology as compared to a corresponding polymer blend.¹⁷ A covalent connection of donor (P3HT) and

SCHEME 5. Synthesis of Poly(3-hexylthiophene)-*b*-poly[9,9-dialkylfluorene]-*b*-poly(3-hexylthiophene) (P3HT-*b*-PF-*b*-P3HT) Triblock Copolymers^a

^a R₁: -2-ethylhexyl or 3,7,11-trimethyldodecyl. R₂: -*n*-hexyl.

SCHEME 6. Synthetic Scheme toward and Structures of All-Conjugated Donor/Acceptor/Donor (DAD)-Type Triblock Copolymers^a

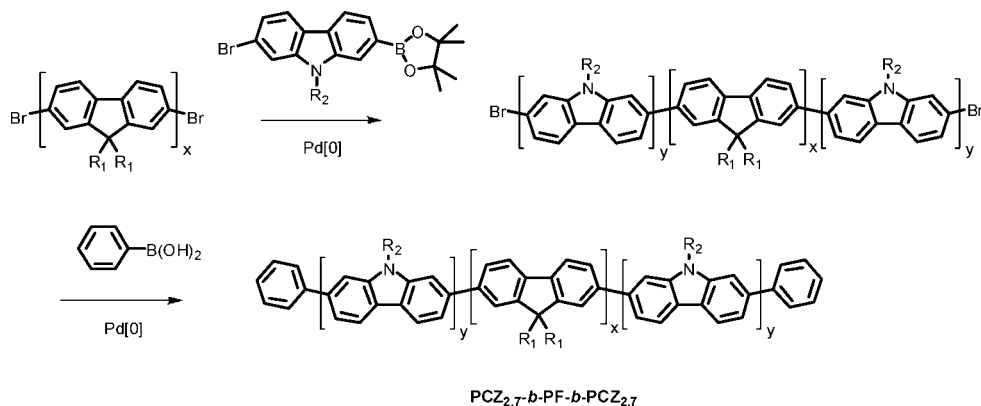
^a Bis-P3HT was generated in a control experiment by coupling two Br-P3HT macromonomers.

acceptor (CN-PPV) blocks seems a favorable way to control the scale length of nanostructure formation.

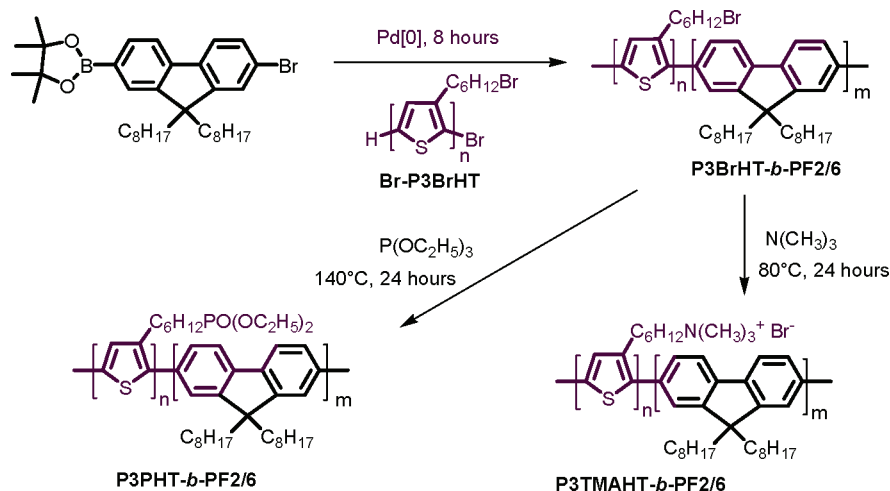
Adapting a similar synthetic approach, Bo and co-workers described in 2007 a series of five all-conjugated ABA-type triblock copolymers containing hole-transporting polycarbazole segments, electron-transporting polyoxadiazole segments, and blue-light-emitting polyfluorene segments in two-step palladium-catalyzed Suzuki-type aryl-aryl cross-coupling protocols [for one example, a poly(*N*-octylcarbazole-2,7-diyl)-*b*-poly(9,9-dioctylfluorene-2,7-diyl)-*b*-poly(*N*-octylcarbazole-2,7-diyl) triblock copolymer (PCZ_{2,7}-*b*-PF-*b*-PCZ_{2,7}); see Scheme 7].¹⁸ Again, dibromoaryl-terminated precursors [polyfluorenes (PFs) or polyoxadiazoles (PODs)] were synthesized first as the central building blocks. Then, the dibromoaryl-terminated pre-

cursors were further reacted with AB-type monomers (2-bromo-9-octylcarbazole-7-pinacolato boronate, 2-bromo-9,9-dioctylfluorene-7-pinacolato boronate) in a "grafting-from" scheme to obtain the target triblock copolymers. The formation of the triblock copolymers was confirmed by gel permeation chromatography (GPC) and NMR spectroscopy. Investigations of the optical properties indicate the occurrence of an efficient intramolecular ("through bond") energy transfer in such triblock copolymers.¹⁸

Extending our previous studies on all-conjugated block copolymers, we investigated the synthesis and nanostructure formation of an AB-type *amphiphilic*, all-conjugated polythiophene-*b*-polyfluorene diblock copolymer containing two conjugated blocks of different polarity in 2007.¹⁹ The idea

SCHEME 7. Synthesis of an All-Conjugated Poly(*N*-octylcarbazole-2,7-diyl)-*b*-poly(9,9-dioctylfluorene-2,7-diyl)-*b*-poly(*N*-octylcarbazole-2,7-diyl) Triblock Copolymer (PCZ_{2,7}-*b*-PF-*b*-PCZ_{2,7}) after Bo et al.^{18a}

^a R₁; R₂, -*n*-octyl.

SCHEME 8. Synthetic Scheme toward the Amphiphilic, All-Conjugated Diblock Copolymer Poly[3-(6-diethylphosphonatohexyl)thiophene]-*b*-poly[9,9-bis(2-ethylhexyl)fluorene] (P3PHT-*b*-PF2/6) and the Ionic Diblock Copolyelectrolyte Poly[9,9-bis(2-ethylhexyl)fluorene]-*b*-poly[3-(6-trimethylammoniumhexyl)thiophene] (P3TMAHT-*b*-PF2/6)

behind this approach was to introduce an additional driving force for self-organization by using conjugated blocks of distinctly different polarity. Following this idea, an amphiphilic, all-conjugated AB-type diblock copolymer P3PHT-*b*-PF2/6, which is composed of a nonpolar, hydrophobic poly[9,9-bis(2-ethylhexyl)fluorene] (PF2/6) and a polar, hydrophilic poly[3-(6-diethylphosphonatohexyl)thiophene] (P3PHT) block, has been synthesized. The switch to AB-type diblock copolymers should further simplify our synthetic procedures and the interpretation of the self-assembly behavior of the diblock copolymer.

Our synthetic approach included three steps (Scheme 8). First, a monobromo-terminated poly[3-(6-bromohexyl)thiophene] (Br-P3BrHT) macromonomer was prepared in a synthetic protocol previously described by McCullough et al. with a mean average molecular weight (M_n) of 19,700 (GPC; PS calibration).²⁰ In the second step, a nonpolar diblock copoly-

mer precursor P3BrHT-*b*-PF2/6 was synthesized under Suzuki cross-coupling conditions with 2-bromo-[9,9-bis(2-ethylhexyl)fluorene]-7-pinacolato boronate as bifunctional AB-type monomer and the monobromo-terminated Br-P3BrHT macromonomer as end-capper (Scheme 8). Afterward, the separation of the target block copolymer and homopolymeric side products was accomplished by several solvent extraction steps which are based on the rather different solubility behavior of the components. The M_n of the hydrophobic, nonpolar diblock copolymer P3BrHT-*b*-PF2/6 was determined to be 29,900, corresponding to an M_n of the PF2/6 block of about 10,000. Within the GPC characterization of P3BrHT-*b*-PF2/6, the detection of the GPC chromatograms was recorded both at 380 and at 450 nm, respectively, corresponding to the long wavelength absorption maxima of the related homopolymers PF2/6 and P3BrHT in dilute solution. The GPC profiles display very similar M_n and M_w values of P3BrHT-*b*-PF2/6 at both detec-

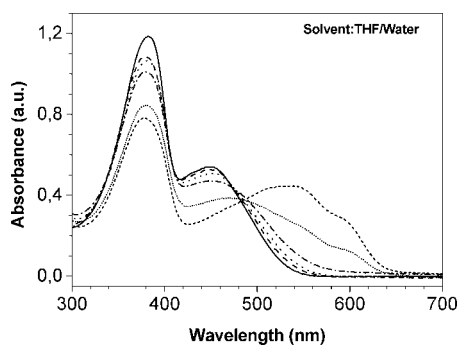


FIGURE 4. Absorption spectra of an amphiphilic diblock copolymer poly[3-(6-diethylphosphonohexyl)thiophene]-*b*-poly[9,9-bis(2-ethylhexyl)fluorene] (P3PHT-*b*-PF2/6) in THF/water mixtures [increasing water concentration: 0 (solid line); 50 (dashed); 60 (dotted); 70 (dash-dotted); 80 (short dotted); 90 (short dashed) %, w/w].

tion wavelengths. This is a clear proof that the resulting material is not a mixture (blend) with one or both homopolymers. Finally, the amphiphilic diblock copolymer P3PHT-*b*-PF2/6 containing both nonpolar, hydrophobic (PF2/6) and polar, hydrophilic blocks (P3PHT) was generated by treating P3BrHT-*b*-PF2/6 with excess triethyl phosphite. P3PHT-*b*-PF2/6 is soluble in THF, chloroform, or acetone (P3BrHT-*b*-PF2/6 is not soluble in acetone!). We could not exactly measure the molecular weight of P3PHT-*b*-PF2/6 by conventional GPC due to the strong interaction of the copolymer with the columns (adsorption).

Figure 4 shows UV-vis spectra of P3PHT-*b*-PF2/6 in dilute solution (THF and THF/water mixtures; polymer concentration: 3.3×10^{-2} mg mL⁻¹). Hereby, pure THF is a nonselective solvent for both blocks. The absorption maximum centered at about 380 nm reflects the absorption of the PF2/6 blocks. The PF2/6 absorption band is relatively insensitive to aggregation processes.²¹ The second absorption maximum at ca. 450 nm in pure THF can be attributed to the absorption of the polar P3PHT blocks. The absorption maximum of the P3PHT block of P3PHT-*b*-PF2/6 at 450 nm is very similar to the absorption maximum of the homopolymer P3PHT in THF. At high water contents of >70%, the polythiophene-related band shows the well-known solvatochromic effect of regio-regular polythiophenes. The λ_{max} value shifts from 450 to 540 nm when increasing the water content in the THF/water mixture. The observed 90 nm red shift indicates an ongoing aggregation of the P3PHT blocks due to the formation of supramolecular aggregates, probably micellar or vesicular particles. As for the solution spectra of the diblock copolymer and the related homopolymers similar λ_{max} values of the absorption maxima of P3PHT-*b*-PF2/6 and P3PHT, respectively, were also found for the aggregated species in THF/water (1:9, v/v)

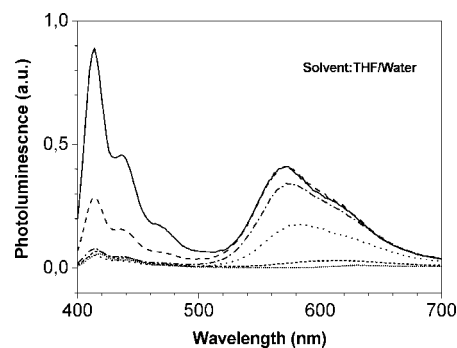


FIGURE 5. Emission spectra of an amphiphilic diblock copolymer poly[3-(6-diethylphosphonohexyl)thiophene]-*b*-poly[9,9-bis(2-ethylhexyl)fluorene] (P3PHT-*b*-PF2/6) in THF/water mixtures [PL excitation, 380 nm; increasing water concentration: 0 (solid line); 20 (dashed); 40 (dash-dotted); 60 (dotted); 80 (short dashed); 90 (short dotted) %, w/w].

or in the solid state (thin film). The distinct isosbestic point observed for the lower energy P3PHT absorption band when increasing the water content indicates the presence of only two distinct species, isolated P3PHT-*b*-PF2/6 chains and aggregates. The red shift of the P3PHT absorption maximum with increasing water content is also documented in a distinct color change from light yellow to purple. The solution UV-vis spectra of P3PHT-*b*-PF2/6 in THF/hexane mixtures display a similar red shift of the absorption maximum λ_{max} of the P3PHT block and a color change with increasing hexane content. Both series of absorption spectra look very similar at first glance. Supramolecular aggregation should occur both for addition of the protic and polar water and for the nonpolar hexane to the initial P3PHT-*b*-PF2/6 solution in THF as nonselective solvent. Absorption spectroscopy alone cannot differentiate between both aggregation processes.

However, photoluminescence spectroscopy gives some deeper insight into the underlying self-assembly processes. When excited into the absorption maximum λ_{max} of the PF2/6 block (380 nm), the photoluminescence (PL) spectra of P3PHT-*b*-PF2/6 in dilute THF solution (concentration: 3.3×10^{-2} mg mL⁻¹) display the expected two series of emission bands at 400–500 nm (PF2/6) and 520–640 nm (P3PHT), respectively (Figure 5). The orange-red emission of the P3PHT block is generated by fluorescence resonance energy transfer (FRET) from the PF2/6 to the P3PHT blocks. The photoluminescence spectra of P3PHT-*b*-PF2/6 in THF/water mixtures show a two-step PL quenching process with increasing amount of water in the solvent mixture. When the ratio of water is increased to 30% (v/v), approximately 90% of the initial photoluminescence from the PF2/6 block is quenched with almost no change of the emission intensity from P3PHT block. While increasing the water content stepwise to 90% (v/v) the lower energy photo-

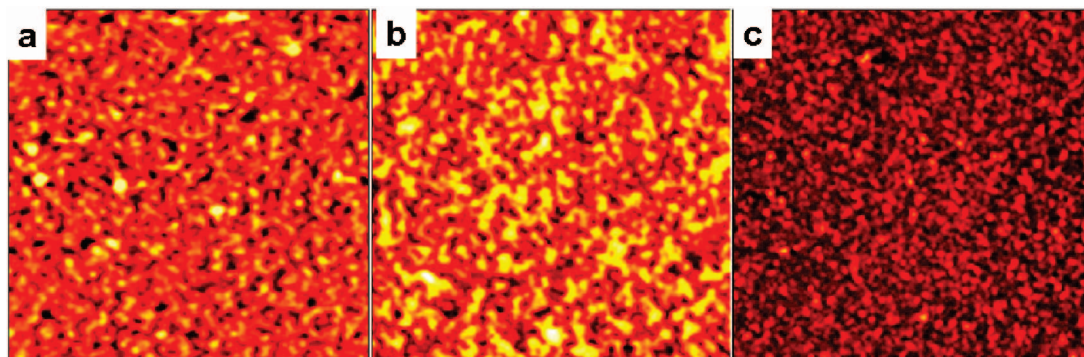


FIGURE 6. AFM images (topography mode) of drop-cast P3PHT-*b*-PF2/6 solutions from THF/water mixtures [a, 30%; b, 80%, c, 90% water; particle size: ca. 140 nm (a, b), 125 nm (c)].

luminescence component of the P3PHT blocks is also quenched. This two-step photoluminescence quenching of P3PHT-*b*-PF2/6 indicates the occurrence of a hierarchical self-assembly process as already discussed during the presentation of the absorption spectra. The block copolymer molecules initially dissolve as individual chains (in THF as nonselective solvent) and self-assemble during the first PL quenching step driven by an aggregation of the PF2/6 segments since their solubility is distinctly reduced with increasing water content. These aggregates should therefore consist of aggregated PF2/6 blocks and nonaggregated P3PHT blocks. THF/water mixtures with low water contents up to 30% (v/v) are still a selective solvent for the hydrophilic P3PHT block. Increasing the water content, also the initially individual P3PHT blocks self-organize into aggregates. The formation of such dense aggregates for water contents of >70% leads to an ongoing photoluminescence quenching also for the P3PHT emission component (Figure 5). This second PL quenching step is accompanied by the already described red shift of the P3PHT absorption band (see Figure 4). Compared with the emission maximum of isolated P3PHT-*b*-PF2/6 chains in THF, the emission maximum of the aggregated P3PHT blocks (90% water) exhibits a red shift of the PL maximum from 570 to 630 nm. The photoluminescence spectra of P3PHT-*b*-PF2/6 in the opposite THF/hexane system (concentration: $3.3 \times 10^{-2} \text{ mg mL}^{-1}$), in contrast to the nearly similar absorption spectra within the THF/water and THF/hexane series, display distinct differences. Increasing the hexane content from 50 to 90% (v/v) the emission of the P3PHT blocks is subsequently quenched without significant changes of the spectral position and intensity of PF2/6-related emission. The PL quenching behavior in this case indicates an aggregation process starting with an agglomeration of the P3PHT blocks. Also high hexane contents (90%) do not lead to a quenching of the PF2/6 emission. Hexane, therefore, is a selective solvent for hydrophobic PF2/6 blocks.

The PL results well correspond to the already discussed UV-vis experiments which showed distinct red shifts of the P3PHT-related absorption bands for hexane contents >60%. The above-described solvent-selective photoluminescence quenching process of P3PHT-*b*-PF2/6 reflects a reversible and controllable supramolecular aggregation in solvents and solvent mixtures of different polarity, which can be used to form preassembled supramolecular ensembles prior to film casting.

Atomic force microscopy (AFM) was used to monitor the morphology of the aggregates in drop-cast films from different solvent mixtures and to estimate the average size of the aggregates, as shown in Figure 6. The contact-mode AFM images clearly indicate that P3PHT-*b*-PF2/6 forms spherical particles (micelles or vesicles) in THF/water mixtures with water contents >30% (Figures 6a–c). The particles display a diameter of approximately 140 nm for water contents of 30–80%, in good agreement with the following light scattering (LS) data. The AFM characterization displays an average height of the particles of only ca. 35 nm. This finding clearly points toward the occurrence of soft particles, probably vesicles. For water contents up to 80% (Figures 6a/b) the particles seem slightly agglomerated after drop casting onto mica, which indicates some interaction of the soft shells (isolated, hydrophilic P3PHT chains). For a water content of $\geq 90\%$ the particles display a small, but significant, reduction of their diameter and do not longer show agglomeration into larger aggregates (Figure 6c). These findings are in full agreement with the discussion of the absorption spectra and the PL quenching results (Figures 4 and 5), showing a red shift of the P3PHT absorption band and a distinct PL quenching of the P3PHT emission (due to aggregation) only for high water contents. Adding the nonpolar hexane to THF solutions of P3PHT-*b*-PF2/6 spherical particles are only observed for high hexane contents of $\geq 80\%$. This result

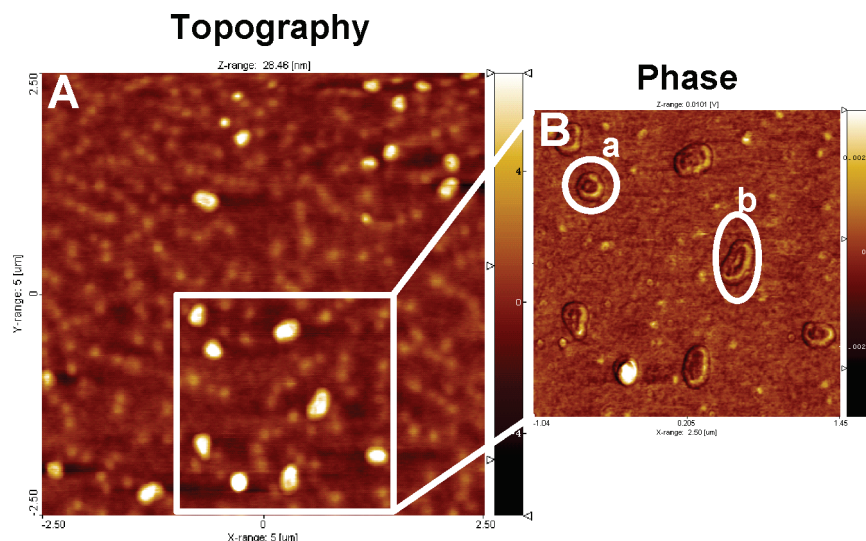


FIGURE 7. (A) AFM topographic and (B) phase image (zoom-in area in A) of PF2/6-*b*-P3PHT Langmuir–Blodgett (LB) films transferred at 5 mN/m. Scan area: (A) $5.0 \times 5.0 \mu\text{m}^2$ and (B) $2.5 \times 2.5 \mu\text{m}^2$.

again supports the discussion of the optical spectra. The average diameter of the “reverse” particles was estimated to about 150 nm.

The interfacial behavior and the resulting surface morphology of our all-conjugated diblock copolymer poly[9,9-bis(2-ethylhexyl)fluorene]-*b*-poly[3-(6-diethylphosphonato)hexyl]thiophene] (PF2/6-*b*-P3PHT) was investigated by a combination of the Langmuir–Blodgett (LB) technique for monolayer formation at the water/air interface, optical spectroscopy, and AFM.²² For PF2/6-*b*-P3PHT diblock copolymer monolayers formed after spreading a chloroform solution at the air/water interface, well-defined gas, liquid-expanded, liquid-condensed, and solid states were observed. At a certain surface pressure the backbones of the polar P3PHT blocks adopt an edge-on arrangement which is driven by the pendant alkyl chains with the polar phosphonate side groups, i.e., the polymer main chain orients parallel to the air/water interface with the planes of the thiophene rings in vertical orientation (edge-on). For comparison of the morphological and optical properties, three different LB films which have been transferred at surface pressures of 5, 15, and 50 mN/m, spin- or drop-cast films, and solutions were investigated. Spectral shifts and intensity changes of UV–vis absorption and photoluminescence spectra of the transferred films were correlated to changes of the surface morphology. The emission properties after excitation into the higher bandgap PF2/6 absorption band were governed both by fluorescence resonance energy transfer (FRET) to and conformational changes within the P3PHT block. The AFM images nicely illustrate the formation of vesicular species at low surface pressures (Figure 7) and their transition into a monolayer lamellar phase upon

increased surface pressure. The diblock copolymer monolayers show a clear correlation of their absorption and emission properties and the aggregation behavior at the air/water interface.²²

Solutions of P3PHT-*b*-PF2/6 in pure THF were also investigated by static and dynamic light scattering (SLS/DLS). Two populations with hydrodynamic radii $R_{h,1}$ of ca. 10 and $R_{h,2}$ of ca. 60 nm, respectively, were found. The smaller species are unimers, which represent the dominant mass fraction in solution. Since light scattering is highly sensitive on large particles, the population of larger size represents only a tiny fraction of the polymer. With the radius of gyration of $R_{g,2} = 60$ nm a characteristic ratio R_g/R_h close to unity is calculated, which is indicative of vesicle formation. The vesicle formation with its relatively low local curvature can be rationalized on the basis of densely packed rod–rod polymers, whereby both blocks exhibit a similar molecular size. The dimensions of the vesicles from SLS/DLS well correspond to the size observed in the AFM investigations. As a conclusion of the optical and morphology investigations Figure 8 gives a schematic illustration of the proposed self-assembly process into vesicular species in THF/water mixtures of different water content.

A next plausible step and extension of our synthetic approach was the generation and characterization of the corresponding ionic analogues to the previously described amphiphilic, all-conjugated block copolymers (P3PHT-*b*-PF2/6) that contain both ionic (polyelectrolyte) and nonpolar blocks.²³ The resulting block polyelectrolytes are expected to exhibit solubility in protic solvents including water and a unique self-assembling behavior which may be reflected in a specific

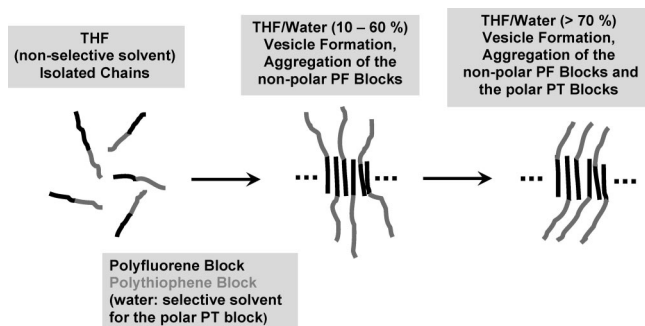


FIGURE 8. Schematic illustration of the vesicle formation in an amphiphilic, all-conjugated block copolymer of the rod-rod type: poly[3-(6-diethylphosphonatohexyl)thiophene]-*b*-poly[9,9-bis(2-ethylhexyl)fluorene] (P3PHT-*b*-PF2/6) in THF/water mixtures of different composition.

response of the optical and electronic properties to specific changes of the surrounding environment. Solubility in water is a crucial prerequisite for a potential use in biosensors (via polyelectrolyte/analyte interactions).

The synthesis of the novel, ionic poly[9,9-bis(2-ethyl-hexyl)-fluorene]-*b*-poly[3-(6-trimethylammoniumhexyl)thiophene] (P3TMAHT-*b*-PF2/6) block copolymer is depicted in Scheme 8 (right). In a first step, again monobromo-terminated poly(3-bromohexylthiophene) (Br-P3BrHT) was prepared, in this case with a mean average molecular weight M_n of ca. 10,000 (corresponding a degree of polymerization D_p of ca. 40) and M_w of ca. 18,000 [polydispersity PD (M_w/M_n): 1.8] in a protocol first described by McCullough et al.²⁰ The second step involves a Suzuki-type cross coupling of 2-bromo-9,9-bis(2-ethylhexyl)fluorene-7-boronic ester using Pd(PPh₃)₄ as catalyst and BrP3BrHT as macromolecular end-capper to synthesize the already described nonpolar diblock copolymer precursor P3BrHT-*b*-PF2/6.¹⁹ The number average molecular weight M_n of the diblock copolymer P3BrHT-*b*-PF2/6 was 18,000, with a M_w of 25,000 and a PD of 1.4. The mean average molecular weight of the PF2/6 block was calculated from the sum molecular weight of the block copolymer P3BrHT-*b*-PF2/6 and the M_n of the polythiophene block (10,000) to 8,000 (D_p : ca. 21). The final polymer-analogous conversion in the synthesis of the cationic diblock copolyelectrolyte P3TMAHT-*b*-PF2/6 involves the quaternization of the 6-bromohexyl functions of the nonionic precursor P3BrHT-*b*-PF2/6 with trimethylamine (Scheme 8).²³

P3TMAHT-*b*-PF2/6 is soluble in polar, protic solvents such as water and methanol. Electrical conductivity studies of P3TMAHT-*b*-PF2/6 in water and methanol point for a higher degree of ionization (dissociation) in water. Absorption/photoluminescence (PL) as well as PL quantum yield (PLQL) measurements indicate the presence of strongly aggregated

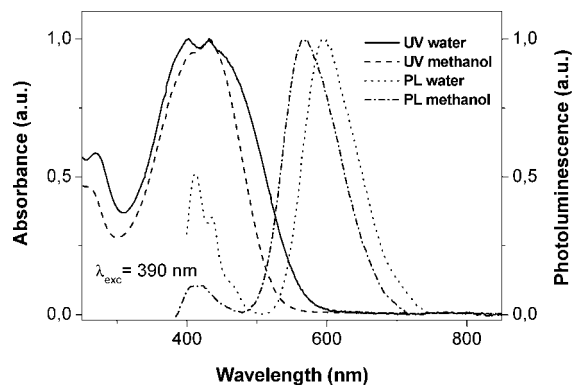


FIGURE 9. UV/vis and photoluminescence (PL) spectra of the diblock copolymer P3TMAHT-*b*-PF2/6 in water and methanol (PL spectra, excitation wavelength, 390 nm).

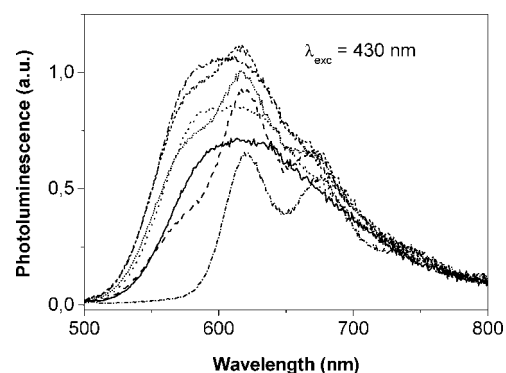


FIGURE 10. Emission spectra of the ionic polythiophene blocks of P3TMAHT-*b*-PF2/6 for the addition of SDS to aqueous solutions of the diblock copolymer [polymer concentration, 2 μM; excitation wavelength, 430 nm; SDS concentration in increasing order: 0 (solid line); 6.4 (dotted); 7.2 (dash-dotted); 10.4 (short dashed); 12.8 (short dotted); 50 (dashed); 160 (short dash-dotted) μM].

species in aqueous solution. An addition of 30–70% THF leads to a subsequent deaggregation which is accompanied by an increased PLQY and a 50 nm blue shift of the emission maximum for the ionic polythiophene block. Both absorption and PL spectra of P3TMAHT-*b*-PF2/6 show spectral signatures of both blocks (Figure 9). Hereby, the large Stokes loss for the ionic polythiophene building block with λ_{\max} (absorption) at ca. 430 and λ_{\max} (emission) at ca. 560 nm (solvent: methanol) documents a distinctly coiled, disordered conformation as driven by the electrostatic repulsion of the charged, cationic side groups. However, the addition of an oppositely charged anionic surfactant sodium dodecyl sulfate (SDS) leads to an ongoing compensation of the charges and to the formation of highly ordered polyelectrolyte/surfactant complexes as indicated by a distinct red shift of the PL maximum (for the polythiophene component) and the occurrence of a well-resolved vibronic structure in the PL band (Figure 10). An AFM investigation of P3TMAHT-*b*-PF2/6 aggregates formed in methanol demonstrates the presence of collapsed vesicu-

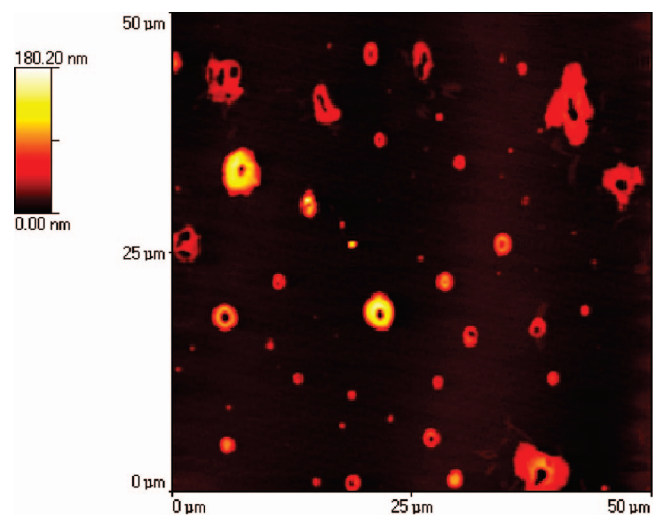


FIGURE 11. AFM image (contact mode) of drop-cast P3TMAHT-*b*-PF2/6 aggregates from methanol onto an untreated glass slide (P3TMAHT-*b*-PF2/6 concentration, 0.03 g/L; average size, 2–5 μm).

lar species with a diameter of ca. 2–5 μm (Figure 11, shown for vesicles formed after drop casting from methanol).²³ Interestingly, drop casting of diblock copolymer P3TMAHT-*b*-PF2/6 from water leads to the formation of aggregates with fractal morphologies as been also observed for other nonconjugated amphiphilic block copolymers (PS-*b*-PEO).²⁴ Future work will be directed to the complexation behavior of P3TMAHT-*b*-PF2/6 with anionic polyelectrolytes as polystyrene sulfonic acid (PSSA) or DNA.

Conclusion

A crucial point in the optimization of organic solar cell materials is a rational control of their nanostructure formation. All-conjugated block copolymers open the unique possibility to engineer materials with tailor-made electronic (fine-tuning of the HOMO and LUMO energy levels of the conjugated blocks) and morphological (solid state morphology of the active layer) properties. Especially di- or triblock copolymers will allow for the organization of these materials into large area ordered arrays with a length scale of nanostructure formation of the order of the exciton diffusion length of organic semiconductors (typically ca. 10 nm).

Only 6 years of initial research into the field of all-conjugated block copolymers have gained a bundle of very promising synthetic approaches and already realized target structures. Especially for amphiphilic diblock copolymers with two blocks of rather different polarity the formation of defined, nanosized supramolecular structures has been observed (micelles, vesicles, lamellar structures) which opens the opportunity for both fundamental and application studies. The combination of the typical block copolymer architectures and the

unique electronic functions of conjugated polymers may result in the development a new generation of organic photovoltaic materials with high solar energy conversion efficiency.

However, a lot of further research is necessary to develop all-conjugated block copolymers with optimized donor/acceptor couples for solar cell applications (showing high open circuit voltage, short circuit current and fill factor). The multiparameter optimization of the block copolymer materials toward an application in organic solar cells must consider both the electronic and morphological (self-assembly) properties.

*The authors would like to thank Prof. Rigoberto Advincula and co-workers, Houston/US (Langmuir–Blodgett films of all-conjugated PF2/6-*b*-P3PHT); Prof. Hugh Burrows and co-workers, Coimbra/Portugal (optical investigations of polyelectrolytes); Prof. Ludwig Josef Balk and co-workers, Wuppertal/Germany (AFM); Prof. Markus Antonietti and Reinhard Sigel, MPIKG Potsdam/Germany (SLS/DLS); and Prof. Dieter Neher and co-workers, Potsdam/Germany (AFM) for a very fruitful and challenging collaboration. The synthetic contributions of Guoli Tu, Heinz-Georg Nothofer, Roland Güntner, Udom Asawapirom, Christopher Schmitt and Michael Forster (Wuppertal) are greatly acknowledged as well as the support in the AFM characterization of the novel block copolymers by Ralf Heiderhoff, Hongbo Li and Sylwia Adamczyk (Wuppertal).*

BIOGRAPHICAL INFORMATION

Prof. Dr. Ullrich Scherf studied chemistry at the Friedrich-Schiller-Universität (Jena, East Germany) and received his Ph.D. in 1988 under the supervision of Prof. Dr. H.-H. Hörhold (synthesis of PPV-type conjugated polymers, carbonization of polymer films). He spent one *postdoc* year at the Institut für Tierphysiologie, Sächsische Akademie der Wissenschaften zu Leipzig (East Germany) in the group of Prof. Dr. H. Penzlin (isolation and characterization of cockroach hormones). After that he joined the MPI for Polymer Research, Mainz, Germany, in 1990 (synthetic polymer chemistry group, Prof. Dr. K. Müllen) and obtained his habilitation from the Johannes-Gutenberg-Universität Mainz, Germany, in 1996 (polyarylene-type ladder polymers). In 1998 he received the Meyer-Struckmann Research Award, in 2000 he became C3-Professor for Polymer Chemistry at the Universität Potsdam, Germany, and in 2002 C4-Professor for Macromolecular Chemistry at the Bergische Universität Wuppertal, Germany. He published ca. 460 papers in refereed journals. Homepage: <http://www2.uni-wuppertal.de/FB9/poly/>.

Andrea Gutacker studied chemistry at the University of Wuppertal and received her Diploma degree in 2007. In October 2007 she started her Ph.D. work in the group of Ullrich Scherf on cationic, conjugated diblock copolymers.

Nils Koenen studied chemistry at the University of Wuppertal and received his Diploma degree in 2006. In February of 2007 he started his Ph.D. work under the supervision of Ullrich Scherf on the synthesis of amphiphilic, all-conjugated diblock copolymers.

FOOTNOTES

*E-mail: scherf@uni-wuppertal.de.

REFERENCES

- Liang, Y.; Wang, H.; Yuan, S.; Lee, Y.; Yu, L. Conjugated block copolymers and oligomers: from supramolecular assembly to molecular electronics. *J. Mater. Chem.* **2007**, *17*, 2183–2194.
- (a) Yokoyama, A.; Miyakoshi, R.; Yokozawa, T. Chain-Growth Polymerization for Poly(3-hexylthiophene) with a Defined Molecular Weight and a Low Polydispersity. *Macromolecules* **2004**, *37*, 1169–1171. (b) Miyakoshi, R.; Shimono, K.; Yokoyama, A.; Yokozawa, T. Catalyst-Transfer Polycondensation for the Synthesis of Poly(*p*-phenylene) with Controlled Molecular Weight and Low Polydispersity. *J. Am. Chem. Soc.* **2006**, *128*, 16012–16013. (c) Yokoyama, A.; Suzuki, H.; Kubota, Y.; Ohuchi, K.; Higashimura, H.; Yokozawa, T. Chain-Growth Polymerization for the Synthesis of Polyfluorene via Suzuki-Miyaura Coupling Reaction from an Externally Added Initiator Unit. *J. Am. Chem. Soc.* **2007**, *129*, 7236–7237.
- Sun, S.; Fan, Z.; Wang, Y.; Haliburton, R.; Taft, C.; Maaref, S.; Seo, K.; Bonner, C. E. Conjugated block copolymers for opto-electronic functions. *Synth. Met.* **2003**, *137*, 883–884.
- Zhang, C.; Choi, S.; Haliburton, J.; Li, R.; Cleveland, T.; Sun, S.; Ledbetter, A.; Bonner, C. Design, Synthesis, and Characterization of a -Donor-Bridge-Acceptor-Bridge- Type Block Copolymer via Alkoxy- and Sulfone- Derivatized Poly(phenylenevinylene)s. *Macromolecules* **2006**, *39*, 4317–4326.
- Sun, S.-S. Design of a block copolymer solar cell. *Sol. Energy Mater. Sol. Cells* **2003**, *79*, 257–264.
- Sun, S.-S.; Zhang, C.; Ledbetter, A.; Choi, S.; Seo, K.; Bonner, C. A.; Drees, M.; Sariciftci, N. S. Photovoltaic enhancement of organic solar cells by a bridged donor-acceptor block copolymer approach. *Appl. Phys. Lett.* **2007**, *90*, 043117.
- Kroeze, J. E.; Savenije, T. J.; Vermeulen, M. J. W.; Warman, J. M. Contactless Determination of the Photoconductivity Action Spectrum, Exciton Diffusion Length, and Charge Separation Efficiency in Polythiophene-Sensitized TiO₂ Bilayers. *J. Phys. Chem. B* **2003**, *107*, 7696–7705.
- Lewis, A. J.; Ruseckas, A.; Gaudin, O. P. M.; Webster, G. R.; Burn, P. L.; Samuel, I. D. W. Singlet exciton diffusion in MEH-PPV films studied by exciton-exciton annihilation. *Org. Electron.* **2006**, *7*, 452–456.
- Haugeneder, A.; Neges, M.; Kallinger, C.; Spirk, W.; Lemmer, U.; Feldmann, J.; Scherf, U.; Harth, E.; Gügel, A.; Müllen, K. Exciton diffusion and dissociation in conjugated polymer/fullerene blends and heterostructures. *Phys. Rev. B* **1999**, *59*, 15346–15351.
- Wang, H. B.; Ng, M.-K.; Wang, L. M.; Yu, L. P.; Lin, B.; Meron, M.; Xiao, Y. Synthesis and Characterization of Conjugated Diblock Copolymers. *Chem.—Eur. J.* **2002**, *8*, 3246–3253.
- Isomura, M.; Misumi, Y.; Masuda, T. Synthesis of an amphiphilic conjugated polymer through block copolymerization of phenylacetylene and (*p*-trityloxycarbonylphenyl)acetylene and the subsequent hydrolysis. *Polym. Bull.* **2001**, *46*, 291–297.
- Schmitt, C.; Nothofer, H.-G.; Falcou, A.; Scherf, U. Conjugated Polyfluorene/Polyaniline Block Copolymers. *Macromol. Rapid Commun.* **2001**, *22*, 624–628.
- Güntner, R.; Asawapirom, U.; Forster, M.; Schmitt, C.; Stiller, B.; Tiersch, B.; Falcou, A.; Nothofer, H.-G.; Scherf, U. Conjugated Polyfluorene/Polyaniline Block Copolymers - Improved Synthesis and Nanostructure Formation. *Thin Solid Films* **2002**, *417*, 1–6.
- Plank, H.; Güntner, R.; Scherf, U.; List, E. J. W. The Influence of Metal Grain Size on Polymer/Metal Bilayer Wrinkling. *Soft Matter* **2007**, *3*, 713–717.
- Plank, H.; Güntner, R.; Scherf, U.; List, E. J. W. Structural and Electronic properties of the First Monolayers of Spin-Cast Polyfluorene-Based Conjugated-Polymer Films. *Adv. Funct. Mater.* **2007**, *17*, 1093–1105.
- Asawapirom, U.; Güntner, R.; Forster, M.; Scherf, U. Semiconding block copolymers - Synthesis and Nanostructure Formation. *Thin Solid Films* **2005**, *477*, 48–52.
- Tu, G.; Li, H.; Forster, M.; Heiderhoff, R.; Balk, L. J.; Scherf, U. Conjugated triblock copolymers containing both electron-donor and electron-acceptor blocks. *Macromolecules* **2006**, *39*, 4327–4331.
- Xiao, X.; Fu, Y.; Sun, M.; Li, L.; Bo, Z. Synthesis and characterization of conjugated triblock copolymers. *J. Polym. Sci., Part A* **2007**, *45*, 2410–2424.
- Tu, G.; Li, H.; Forster, M.; Heiderhoff, R.; Sigel, R.; Balk, L. J.; Scherf, U. Amphiphilic, Conjugated Block Copolymers - Synthesis and Solvent-Selective Photoluminescence Quenching. *SMALL* **2007**, *3*, 1001–1006.
- Zhai, L.; McCullough, R. Layer-by-layer Assembly of Polythiophene. *Adv. Mater.* **2002**, *14*, 901–905.
- Scherf, U.; List, E. J. W. Semiconducting Polyfluorenes - Towards Reliable Structure-Property-Relations. *Adv. Mater.* **2002**, *14*, 477–487.
- Park, J. Y.; Koenen, N.; Ponnampati, R.; Forster, M.; Scherf, U.; Advincula, R. Vesicle formation and fusion into a monolayer lamellar phase of an amphiphilic polyfluorene-*b*-polythiophene diblock copolymer at the air-water interface. *Macromolecules* **2008**, *41*, in press.
- Gutacker, A.; Koenen, N.; Adamczyk, S.; Scherf, U.; Pina, J.; Fonseca, S. M.; Seixas de Melo, J.; Valente, A. J. M.; Burrows, H. D. Synthesis, photophysics and solution behaviour of cationic fluorene-thiophene diblock copolymers. *Macromol. Rapid Commun.* **2008**, *29*, F50–F51.
- Peng, J.; Han, Y.; Knoll, W.; Kim, D. H. Development of nanodomain and fractal morphologies in solvent annealed block copolymer thin films. *Macromol. Rapid Commun.* **2007**, *28*, 1422–1428.